Original Research

Irisin induces white adipose tissue browning in mice as assessed by magnetic resonance imaging

Yue Chen[1], Jie Ding[1], Yufei Zhao[1], Shenghong Ju[1], Hui Mao[2] and Xin-Gui Peng[1]

[1]Jiangsu Key Laboratory of Molecular and Functional Imaging, Department of Radiology, Zhongda Hospital, Medical School, Southeast University, Nanjing 210009, P. R. China; [2]Department of Radiology and Imaging Sciences, Emory University, Atlanta, GA 30322-1007, USA

Corresponding author: Xin-Gui Peng. Email: xingui2005peng@126.com

Impact statement

Irisin can be used to activate and facilitate browning of WAT for treating obesity-related metabolic diseases and disorders. MRI is capable of noninvasively monitoring the process of WAT browning and the effect of irisin intervention.

Abstract

This study aimed to track and evaluate the effect of low-dose irisin on the browning of white adipose tissue (WAT) in mice using magnetic resonance imaging (MRI) noninvasively *in vivo*. Mature white adipocytes extracted from mice were cultured, induced and characterized before being treated by irisin. The volume and fat fraction of WAT were quantified using MRI in normal chow diet and high fat mice after injection of irisin. The browning of cultured white adipocytes and WAT in mice were validated by immunohistochemistry and western blotting for uncoupling protein 1 (UCP1) and deiodinase type II (DIO2). The serum indexes were examined with high fat diet after irisin intervention. UCP1 and DIO2 in adipocytes showed increases responding to the irisin treatment. The size of white adipocytes in mice receiving irisin intervention was reduced. MRI measured volumes and fat fraction of WAT were significantly lower after Irisin treatment. Blood glucose and cholesterol levels were reduced in high fat diet mice after irisin treatment. Irisin intervention exerted browning of WAT, resulting reduction of volume and fat fraction of WAT as measured by MRI. Furthermore, it improved the condition of mice with diet-induced obesity and related metabolic disorders.

Keywords: Obesity, adipocytes, white, uncoupling protein 1, metabolic diseases

***Experimental Biology and Medicine* 2021; 246: 1597–1606. DOI: 10.1177/15353702211006049**

Introduction

The increasing prevalence of obesity and defective adipose tissue function are inextricably linked to the development of metabolic diseases such as type 2 diabetes.[1,2] In addition to white adipocytes and brown adipocytes, the "brown-like" beige adipocytes within white adipose tissue (WAT) found in both mouse and human[3] are derived from MYF5-negative white fat, which, like classical brown adipocytes, respond to cyclic AMP stimuli with a high level of uncoupling protein 1 (UCP1) expression and respiratory rate.[4,5] Evidence has shown that brown and beige adipocytes make significant contributions to systemic energy expenditure and regulation of metabolic homeostasis.[6,7] It is possible to control and treat obesity and diabetes by induction of the beige adipocytes in WAT.[8]

Irisin, a hormone secreted by muscle,[9] is produced by cleavage and modification of fibronectin type III domain containing protein 5.[10] Irisin acts on white adipocytes to stimulate UCP1 expression and browning.[11] Even more, a slight increase in the level of irisin in the blood resulted in an increase in the energy expenditure by exercise in mice without change in food intake,[12] raising the question whether irisin could modulate glucose homeostasis and exert the pharmaceutic effect to control the obesity.[13] Interestingly, irisin in mice and humans is 100% identical, suggesting its highly conserved function.[13,14]

Noninvasive measurement of a specific type of adipose tissue and its distribution is of great significance for monitoring metabolic diseases and their treatment.[15] Imaging technologies such as contrast-enhanced ultrasound, positron emission tomography (PET), and magnetic resonance imaging (MRI) are currently used for determining the fatty tissue and contents in both research and clinical applications. Compared to ultrasound and PET, MRI offers high

spatial resolution and soft-tissue contrast with capability of spectroscopically detecting and quantifying specific metabolites without introducing radiation.[16] T1-weighted imaging is commonly used to distinguish WAT from others and can be used to measure the volume of WAT.[17] Chemical shift-selective imaging (CSSI) can be tuned to the specific chemical shift or frequency of fat components to detect changes in the fat fraction (FF).[18] In the past, the effect of irisin on browning process of WAT was only investigated *ex vivo* by traditional molecular biology and pathology techniques. Herein, we report the noninvasive *in vivo* tracking and evaluation of the dose-dependent effect of irisin on the browning of WAT in mice using MRI.

Materials and methods

Culture and identification of primary white adipocyte. All animal studies were approved by Institutional Animal Care and Bioethical Committee of the Medical school of Southeast University (SYXK2016-0014). Mature primary adipocytes were cultured and induced as previously described.[19] After C57/BLKS/J male mice ($n = 2$, 3–4 weeks) were sacrificed by excessive anesthesia, the inguinal subcutaneous adipose tissue (sWAT) was dissected, washed with PBS (Hyclone, Logan, Utah, USA), minced 1–2 mm and digested in PBS containing collagenase II (1 mg·mL^{-1}, Sigma–Aldrich, USA) for 90 min at 37°C. Digested tissue was filtered and centrifuged at 1000 r/min for 5 min to pellet the stroma-vascular cells. The pellets were then resuspended in Dulbecco's Modified Eagle (DMEM/F12, Gibco, Paisley, UK) supplemented with 10% fetal bovine serum (FBS, Gibco, Paisley, UK). The cells proliferated to fill the cell culture dish more than 80%, then induced for three days by an adipogenic cocktail containing 1 μM dexamethasone, 5 μg mL^{-1} insulin, 1 μM rosiglitazone, and 0.5 μM isobutylmethylxanthine in adipocyte culture medium. Three days after induction, cells were maintained in adipocyte culture medium containing 5 μg mL^{-1} insulin and 1 μM rosiglitazone. Finally, cells were incubated in the adipocyte culture medium and harvested. Mature adipocytes were characterized by Oil Red O (Sigma–Aldrich, USA) staining, which confirmed the adipocyte differentiation. Preparation of 60% isopropanol solution: 98% isopropanol (60 mL) was added into distilled water (40 mL) and mixed. Preparation of oil red O staining solution: 100 mL of 100% isopropanol was added with 0.5 g of oil red O dry powder to fully dissolve and filter. The oil red O staining solution mentioned above and distilled water were diluted at 3:2 and filtered (filter paper or polar filter film with 1 mL syringe).

Culture medium was discarded carefully and gently, rinsed with pre-cooled PBS for three times, added 10% neutral formaldehyde and fixed it for 30 min. Oil red O dye solution was added for 0.5 h. About 60% isopropanol was used to decolorize. Selected sections were examined in 5 min with inverted microscopy (IX71, Olympus, Tokyo, Japan) for lipid deposition analysis.

Irisin intervention and evaluation. Cultured white adipocytes were treated with irisin (R&D systems, USA) at different concentrations (0, 20, and 40 nmol·L^{-1}) for six-days. After the treatment, the cells immunohistochemical staining was performed as before.[20]

Proteins were extracted from cultured cells and immunoblotting was processed as previously described.[21] Specific experimental steps were located at supplemental materials.

Mouse model and irisin intervention. Male C57BLKS/J mice were randomized to feed a normal chow diet (NCD) or a high fat diet (HFD) and were housed in standard cages at a temperature of 22–24°C with a 12-hour light/dark cycle. The sources of HFD and NCD are provided directly by the mouse purchase center. NCD mice were fed with normal food directly, while HFD mice were fed with high-fat food (Research Diets, #D12492, USA) and normal food in the ratio of 6:4 for three months. High-fat food was composed of protein (20% kcal), carbohydrate (26.3% kcal), and fat (60% kcal). NCD mice ($n = 24$, 10–12 weeks, 28.07 ± 1.36 g) and HFD mice ($n = 10$, 20–22 weeks, 42.94 ± 4.31g) were randomized into the irisin treatment group and control group. NCD ($n = 12$, 28.23 ± 1.17 g) or HFD ($n = 5$, 43.31 ± 3.15 g) mice were treated daily with irisin (0.8 ng·g^{-1}·day^{-1}, 200 μL each) by intraperitoneal injection for 14 days, while NCD ($n = 12$, 27.92 ± 1.52 g) or HFD ($n = 5$, 42.56 ± 5.20 g) mice in the control group were given phosphate-buffered saline (PBS; 200 μL each) daily at the same volume. Food intake and body weight of mice were monitored at regular intervals every day.

MRI scan and image analysis. After intervention, the two groups of NCD mice and two groups of HFD mice were scanned with MRI ($n = 5$/group). MRI examinations were performed at day 15 after irisin treatment on a preclinical 7 T MR imager (Bruker Pharma Scan MRI, Ettlingen, Germany) using a transmit-receiver quadrature volume coil. The animals were anesthetized by inhalation of a mixture of air and 5% isoflurane (Keyue, Shandong, China) delivered through a nose cone, and anesthesia was maintained with 1–2% isoflurane during MRI scan.

T1-weighted spin echo images were acquired with a multislice multiecho sequence in the axial direction. See the supplementary document for T1-weighted scanning parameters. No fat suppression and slice spacing were used. WAT includes subcutaneous WAT (sWAT) and visceral WAT (vWAT). The sWAT is found mostly underneath the skin. The vWAT, also known as organ fat, is located inside the peritoneal cavity packed in between the internal organs. The volume of sWAT, epididymal WAT (eWAT), vWAT, and total WAT (tWAT) in the whole body of mice were measured and analyzed. The WAT volume was measured using ImageJ software (National Institutes of Health, USA). T1-weighted analysis by Image J software was conducted on the whole volume on manually sketching.

See the supplementary document for data acquisition parameters of CSSI. A region of interest (ROI) was placed at the site of the WAT in both fat and water images. ROIs contained 15–20 pixels (about 0.25 mm^2) for sWAT

in inguinal region, eWAT, eWAT was chosen as the representative of vWAT, because eWAT was relatively concentrated, which could reduce the measurement error. The signal intensity (SI) in the ROI was measured using a program (ParaVision5.0; Bruker PharmaScan) from both fat selective images (SI_{fat}) and water selective images (SI_{water}). FF of WAT was computed following the equation

$$FF_{CCSI} = 100 \times SI_{fat}/(SI_{fat} + SI_{water} \times R) \quad (1)$$

R is the ratio of the fat-to-water proton densities in their pure form, which has a value of 0.9 as used in the early publication.[18]

Histopathologic analysis. After imaging experiments, mice ($n = 5$/group) were sacrificed and then did cardiac perfusion with phosphate-buffered saline and 4% paraformaldehyde in 0.1 M phosphate buffer (pH 7.4). The sWAT and eWAT sections were fixed for 48 h, then dehydrated, embedded, and transversely cut into 4-μm-thick sections for hematoxylin and eosin (H&E) staining.[21] The areas such as blood vessels, were manually excluded by a pathologist.

Five random fields in the microscopic images of H&E staining sections from each mouse were captured. The area of adipocytes was measured using ImageJ software.

Immunohistochemistry analysis and western blotting. Portions of the sWAT samples of irisin treatment group and the control group ($n = 3$/group) in NCD and HFD mice were harvested for immunohistochemistry staining or western blot. See the supplementary document for specific steps.

Measurement of blood glucose, plasma triglyceride, total cholesterol

Mice with HFD were fasted for 24 h. For blood sample analysis, a 500 μL of blood sample was collected from each HFD mouse ($n = 5$/group). Samples were centrifuged, and plasma was stored at −70°C. Glucose, total cholesterol, and triglyceride concentrations in the blood as well as urea and blood nitrogen levels were measured by the autoanalyzer (Au5821, Beckman Coulter, USA).

Statistical analysis

All statistical analyses were performed using SPSS software (SPSS for Windows, version 11.0, 2001; SPSS, Chicago, IL). Numerical data were presented as the mean ± standard deviation (SD). For statistical comparisons, the independent-sample *t*-test and one-way ANOVA were applied. A *P* value of less than 0.05 was considered to indicate a statistically difference.

In cell experiments, one-way ANOVA was used to evaluate the expression of browning protein after treatment using three different irisin concentrations. In animal experiments, independent-sample *t*-test was performed to analyze the body weight, food intake, volume and FF of WAT measured by MRI, and their data of histopathologic and western blotting between irisin treatment and control groups.

Results

Irisin caused browning primary white adipocytes

To investigate the effect of irisin on browning the white adipose adipocyte, we first examined cultured primary white adipocytes derived from C57/BLKS/J male mice. Primary vascular stromal cells were fusiform adherent and fused up to 80%. After six days of induction and two-days of basic culture, the cells began to show lipid droplets of different sizes (Figure 1(a)). The characteristics of primary white adipocytes with the absorption of oil red O by lipid droplets can be seen in the microscope (scale bar = 20 μm; Figure 1(b)).

After treatment, immunohistochemistry analysis showed a significant upregulation of UCP1, the brown adipocyte marker, in primary white adipocytes treated with irisin ($P < 0.05$) compared with the controls treated with PBS. UCP1 was identified in the form of intracellular expression. Moreover, quantification of UCP1 revealed that the upregulation as the concentration of irisin increased (scale bar = 50 μm) (Figure 1(c)). The treatment response at the protein level evidenced with increase in DIO2 content in primary white adipocytes was also confirmed by the Western blotting (Figure 1(d)). Significant increases of DIO2 were seen in white adipocytes after irisin intervention ($P < 0.01$) compared to the controls treated with PBS (Figure 1(d)).

Irisin led to weight loss in NCD mice without changing food intake

We found no statistically significant difference in food intake between the NCD mice treated with irisin ($n = 12$/group) or PBS ($P > 0.05$; Appendix 1, Supplementary Figure S1A). However, irisin-treated mice appeared to be resistant to the weight gain during the experiment period compared to the controls (Appendix 1, Supplementary Figure S1B). The average weight of the irisin-treated group (27.54 ± 1.60 g) was lower than mice treated with PBS (28.23 ± 1.58 g) at the end of the experiments. The averaged change of weight was −0.69 ± 0.99 g in the irisin-treated group during the treatment comparing to 0.31 ± 0.54 g in the control group treated with PBS ($P < 0.01$) (Appendix 1, Supplementary Figure S1C).

Irisin promoted WAT browning as measured by MRI in vivo in NCD mice

We used two different MRI methods to individually measure the volume and FF of WAT in the NCD mice ($n = 5$/group) noninvasively. T1-weighted spin echo imaging was used to measure the volume of sWAT, eWAT, vWAT, and total WAT (tWAT), while CSSI was used to determine the FF of sWAT and eWAT. The MRI measured volumes of sWAT, eWAT, vWAT, and tWAT deposits in mice with irisin intervention are 0.86 ± 0.42 cm^3, 0.46 ± 0.26 cm^3, 0.81 ± 0.34 cm^3, and 1.67 ± 0.74 cm^3, respectively, which are significantly

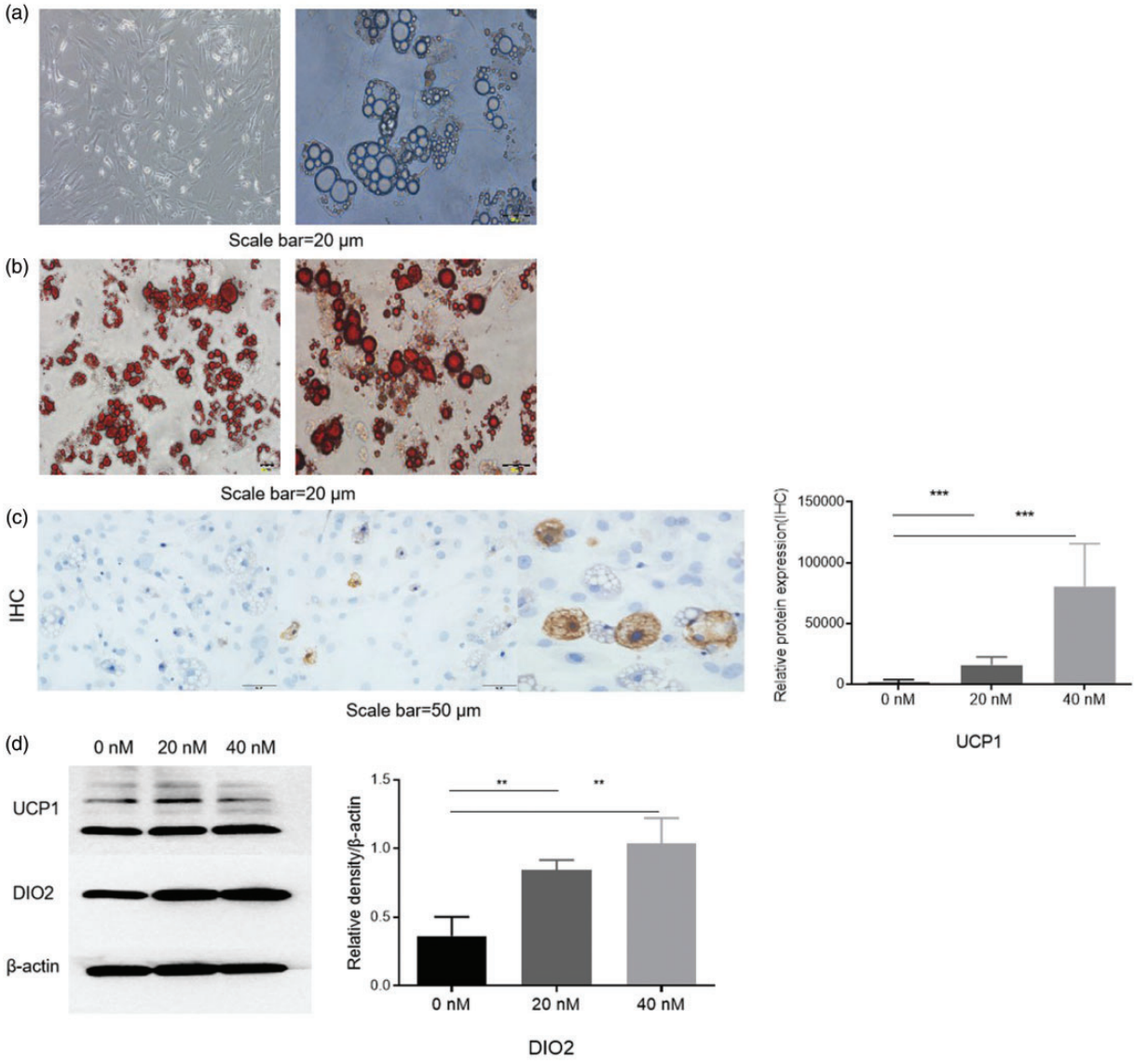

Figure 1. Microscopic images of primary white adipose cells and browning of white adipocytes after applying irisin at different concentrations. Morphology of primary white adipose precursor cells (scale bar=50 μm), a large amount of lipid droplets after induction of maturity (scale bar=20 μm) (a); high magnification at 200× and at 400× of mature fat cells are stained with oil red O, and the lipid droplets appear as orange-red of different sizes (scale bar=20 μm) (b). Immunohistochemistry staining of UCP1 protein mainly expressed in the cytoplasm (scale bar=50 μm) and the content of UCP1 increased significantly with the increase of irisin concentration (c). Western blot showed after irisin intervention at 20 and 40 nmol/L, the gray scale of UCP1 and DIO2 bands was significantly enhanced due to sWAT browning. With the increase of irisin concentration, the expression of DIO2 was also increased (d). (A color version of this figure is available in the online journal.)
UCP1: uncoupling protein 1; DIO2: deiodinase II (*$P < 0.05$, **$P < 0.01$, ***$P < 0.001$).

lower than those in animals of the control groups, i.e. $1.52 \pm 0.22\,cm^3$, $0.79 \pm 0.20\,cm^3$, $1.24 \pm 0.27\,cm^3$, $2.76 \pm 0.31\,cm^3$, respectively (Figure 2(a) and (b)). Furthermore, the selective water imaging and fat imaging with CSSI allowed for measuring FFs of sWAT and eWAT. Analyzing CSSI data revealed that mice with irisin intervention had lower FF of sWAT ($77.82 \pm 1.53\%$) than that of controls ($81.42 \pm 1.64\%$) as shown in Figure 2(c) and (d). Meanwhile, FF of eWAT in mice after irisin intervention was $80.20 \pm 1.80\%$, which is statistically significant lower than that of controls ($82.62 \pm 0.74\%$; Figure 2(e) and (f)). These findings suggested that the irisin treatment not only reduced the overall volume of fat tissue in different compartments, but also decreased FF of WAT.

H&E staining confirmed that the sizes of white adipocytes in sWAT of NCD mice ($n = 3$) treated with irisin intervention (Figure 3(a)) were significantly smaller than those of the control group (Figure 3(b), $P < 0.05$). No lipid droplet change was present in eWAT of mice treated with irisin (Figure 3(c) and (d)). Immunohistochemistry showed that the UCP1 and DIO2 proteins were present in fat cytoplasm (Figure 3(e) and (g)). Similarly, contents of UCP1 and DIO2 proteins were significantly increased in mice ($n = 3$) receiving irisin intervention. The brown-type color features of sWAT were evidenced by the presence of much more abundant multilocular UCP1-positive, DIO2-positive beige adipocytes in sWAT (Figure 3(f), $P < 0.001$; Figure 3(h), $P < 0.01$). Additionally, upregulation of UCP1 and DIO2

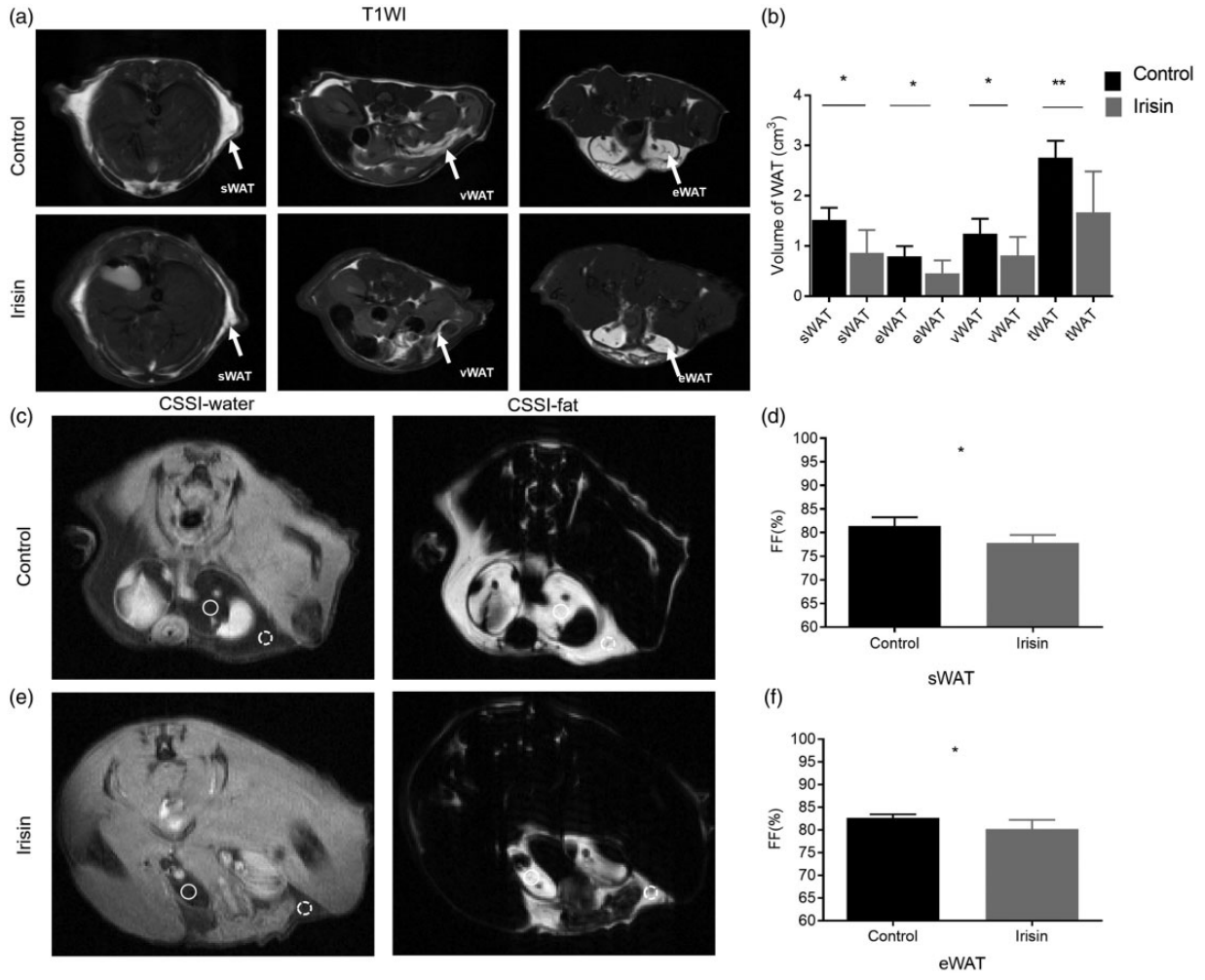

Figure 2. MRI measured *in vivo* change in the WAT after irisin intervention in NCD mice. T1-weighted images show that the subcutaneous, epididymal, visceral and total WAT (a), white arrows indicated the location of each fat pad; after irisin intervention, the volume of each fat pad in mice decreased significantly (b). The selective water imaging (left) and fat imaging (right) with two sequences of CSSI show the different contrasts and signal intensities of sWAT (c) and eWAT (e) of the mice in different groups. Quantitative analysis reveals statistically significant difference in the FF between the two groups of mice (d, f). ROIs are indicated with white circles. WAT: white adipose tissue; FF: fat fraction; CSSI: chemical shift-selective imaging; sWAT: subcutaneous white adipose tissue; eWAT: epididymis white adipose tissue; ROI: region of interest. (*$P < 0.05$, **$P < 0.01$)

was observed in the western blot ($n = 3$) (Figure 3(i)) in NCD mice treated with irisin.

Irisin ameliorated obesity and metabolic dysfunction in HFD mice

To further determine the effect of irisin on diet-induced obesity, we treated C57BLKS/J mice under HFD (male, $n = 5$) with irisin. The HFD mice had significantly higher averaged body weight than NCD mice at the age of 20–22 weeks (42.94 ± 4.31 g vs. 28.02 ± 0.29 g; Appendix 1, Supplementary Figure S2A). There was no statistical difference in the food intake between irisin treatment group and control group during three months of HFD challenge (Appendix 1, Supplementary Figure S2B). However, after the irisin treatment for 14 days, the averaged body weight of the treated animals (44.61 ± 4.28 g) was found to be significantly lower than that of the control group (48.17 ± 4.32 g; Appendix 1, Supplementary Figure S2(c) and (d)).

The MRI measured volumes of sWAT, eWAT, vWAT, and tWAT deposits in mice with irisin intervention are $3.85 \pm 0.63\,cm^3$, $0.84 \pm 0.39\,cm^3$, $7.82 \pm 1.55\,cm^3$, and $12.51 \pm 1.97\,cm^3$, respectively, which are significantly lower than those in animals of the control groups, i.e. $5.55 \pm 0.66\,cm^3$, $1.64 \pm 0.31\,cm^3$, $12.37 \pm 2.49\,cm^3$, and $19.56 \pm 3.39\,cm^3$, respectively (Figure 4(a) and (b)). Furthermore, analyzing CSSI data revealed that mice with irisin intervention had lower FF of sWAT ($77.08 \pm 2.96\%$) than that of controls ($81.75 \pm 1.75\%$) as shown in Figure 4(c) and (d). Meanwhile, FF of eWAT in mice after irisin intervention was lower than that of controls ($75.78 \pm 5.01\%$, $81.55 \pm 2.22\%$, respectively; Figure 4(e) and (f)). These findings suggested that the irisin treatment not only reduced the overall volume of fat tissue in different compartments, but also decreased FF of WAT.

H&E staining confirmed that the sizes of white adipocytes in sWAT and eWAT of HFD mice ($n = 5$) treated with irisin intervention were significantly smaller than those of

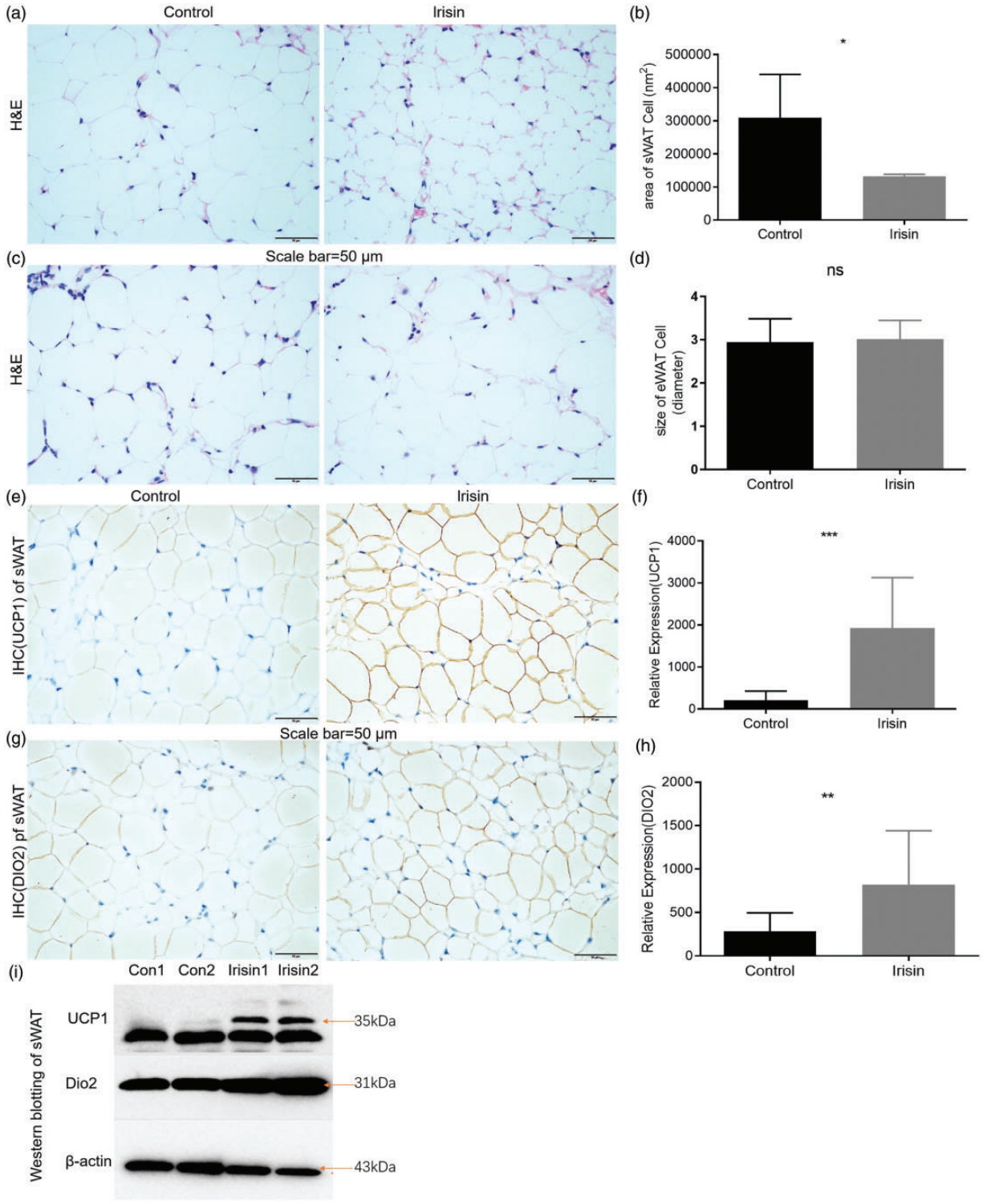

Figure 3. Changes of lipid droplets and immunohistochemistry analysis of specific protein in NCD mice. The morphological changes of adipocytes in WAT (scale bar=50 μm) can be observed, left image showed the WAT in control, and right image was the WAT after irisin treatment (a, c), with size and area of adipocytes in sWAT significantly reduced (b) in mice received irisin intervention. While there is no difference between the size and diameter in eWAT of two groups (d). Immunohistochemistry analysis showed the content of white adipose tissue-associated specific proteins UCP1 and DIO2 (scale bar=50 μm) in the sWAT and increases in irisin group (e–h). Expression levels of UCP1 and DIO2 proteins were significantly increased (I). (A color version of this figure is available in the online journal.)

WAT: white adipose tissue; sWAT: subcutaneous white adipose tissue; eWAT: epididymis white adipose tissue; UCP1: uncoupling protein 1; DIO2: deiodinase II (*ns*, $P > 0.05$, *$P < 0.05$, **$P < 0.01$, ***$P < 0.001$).

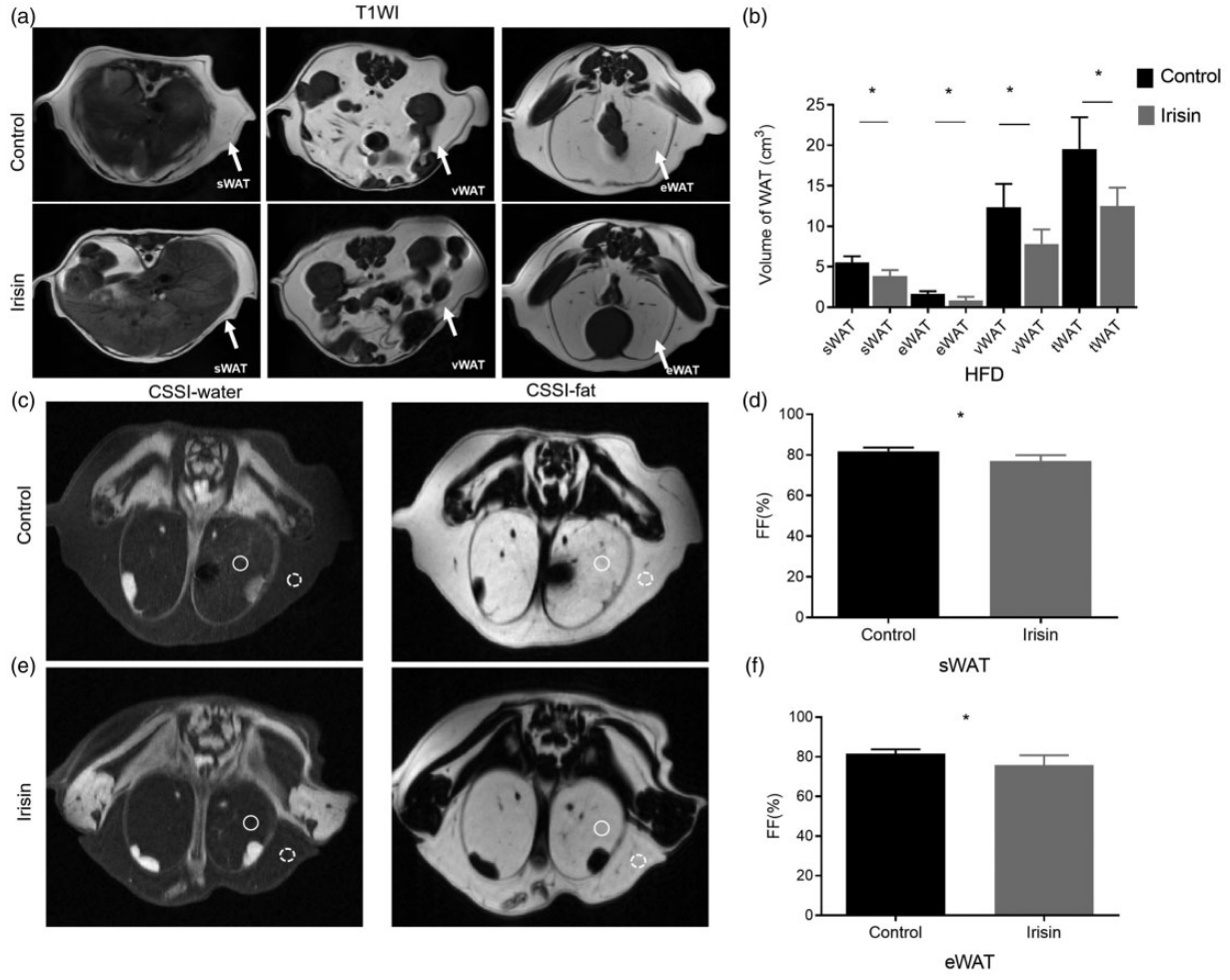

Figure 4. MRI measured in vivo change in the WAT volume and FF in HFD mice. T1-weighted images show that the subcutaneous, epididymal, visceral and total WAT (a), white arrows indicated the location of each fat pad; after irisin intervention, the volume of each fat pad in mice decreased significantly (b). The selective water imaging (left) and fat imaging (right) with two sequences of CSSI show the different contrasts and signal intensities of sWAT (c) and eWAT (e) of the mice in different groups. Quantitative analysis reveals statistically significant difference in the FF between the two groups of mice (d, f). ROIs in sWAT are indicated with white dot line circles, ROIs in eWAT are indicated with white solid line circles.
WAT: white adipose tissue. FF: fat fraction; CSSI: chemical shift-selective imaging; sWAT: subcutaneous white adipose tissue; eWAT: epididymis white adipose tissue; ROI: region of interest. (*$P < 0.05$).

the control group (Figure 5(a) and (b), $P < 0.01$). Immunohistochemistry showed that the UCP1 protein significantly increased in mice ($n = 5$) receiving irisin intervention. The brown-type color features of sWAT and eWAT were evidenced by the presence of much more abundant multilocular UCP1-positive beige adipocytes (Figure 5(c), $P < 0.05$; Figure 5(d), $P < 0.01$).

Moreover, when evaluating the metabolism of the serum metabolic profile, HFD mice with irisin treatment exhibited a lower fasting blood glucose level ($7.72 \pm 1.13\,\text{mmol}\cdot\text{L}^{-1}$) and a total cholesterol level ($2.55 \pm 0.40\,\text{mmol}\cdot\text{L}^{-1}$), comparing to those treated with PBS (glucose level $= 12.88 \pm 2.01\,\text{mmol}\cdot\text{L}^{-1}$, total cholesterol level $= 3.77 \pm 0.76\,\text{mmol}\cdot\text{L}^{-1}$) as shown in Figure 5(e) and (f). Interestingly, there was no change in the triglyceride level (Figure 5(g)).

Discussion

The main finding of our study was that a small dose of irisin can induce browning primary white adipocytes and weight loss in NCD and HFD mice without changing food intake. Furthermore, the irisin treatment may ameliorate obesity and metabolic dysfunction. We demonstrated that treatment induced change of WAT browning can be measured by noninvasive MRI *in vivo*.

Many studies confirmed that irisin acts on white adipocytes and induces their transformation into beige adipocytes. Activated beige adipocytes increase heat production by rapidly consuming glucose and fat, thereby promoting weight loss and improving glucose tolerance and insulin resistance.[22] Some studies showed that the irisin level can be increased by exercise and FNDC-associated virus injection that expresses irisin.[23] Other studies reported the effective response by administering irisin at higher doses ($100\,\text{mg}\cdot\text{kg}^{-1}\cdot\text{d}^{-1}$, 4 weeks).[24] In our study, we observed that the browning primary white adipocytes can be achieved at low-dose irisin (20 nM) in vitro and $0.8\,\text{ng}\cdot\text{g}\cdot\text{d}^{-1}$ in vivo by intraperitoneal injection for 14 days.

We demonstrated that noninvasive MRI can be readily used to quantitatively assess the distributions of fat as a

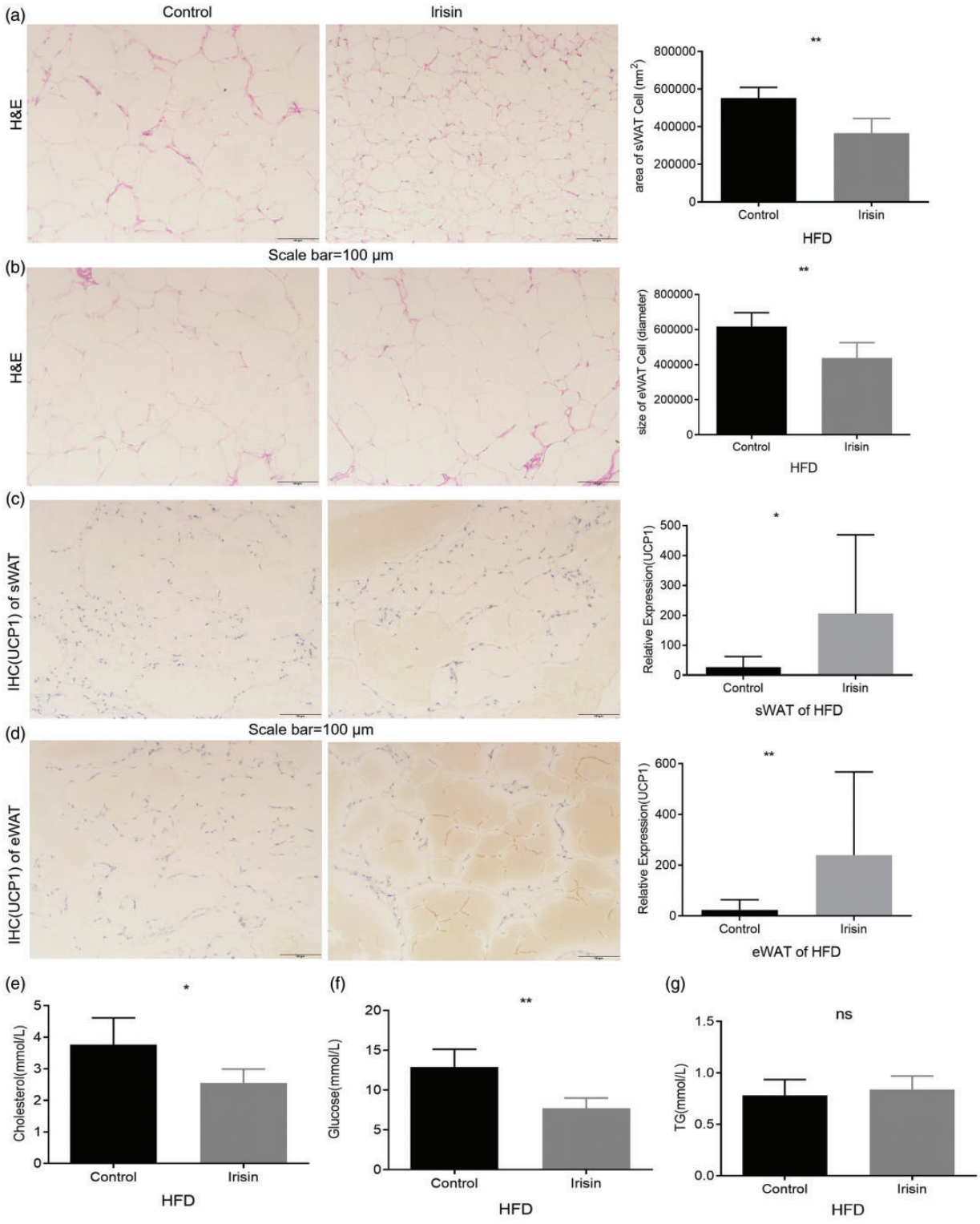

Figure 5. Changes of lipid droplets, specific protein of WAT and metabolic dysfunction after intervention in HFD mice. The morphological changes of adipocytes in WAT (scale bar=100 μm) can be observed, with area of adipocytes in sWAT and eWAT significantly reduced (a, b) in mice received irisin intervention. Immunohistochemistry analysis showed the content of WAT-associated specific proteins UCP1 (scale bar=100 μm) in the sWAT and eWAT (c, d). Fasting cholesterol and blood glucose levels in the experimental group were significantly lower than those in the control group with statistical significance (e, f). There were no significant changes in triglycerides between treated and control mice (g). (A color version of this figure is available in the online journal.)
WAT: white adipose tissue. sWAT: subcutaneous white adipose tissue; eWAT: epididymis white adipose tissue. HFD: high fat diet; PBS: phosphate-buffered saline (ns, $P > 0.05$, $^{*}P < 0.05$, $^{**}P < 0.0$, $^{***}P < 0.001$).

whole and as specific sub-types with good spatial resolution. The imaging methods provide a wide range of coverage of WAT, and ability to quantitatively analyze the FF of WAT in each region. CSSI offers noninvasive method to quantify the FF, which acquires separate fat and water images based on the frequencies of the protons from fat and water in our previous study. During the browning process of WAT, the fat content of WAT decreased, consequently the water increased, so the FF data of the CSSI decreases.[16] Therefore, quantitative analysis of FF value by MRI can judge the change of fat properties. Our study demonstrated that the browning of WAT was detected by CSSI noninvasively, due to the reduction of white adipocyte size and lipid droplets after irisin intervention. Comparing to traditional molecular biology and histopathology analyses on the tissue samples in the past, the imaging approach enables time-dependent monitoring the pharmaceutical effects in the same animal over the time. We showed that T1-weighted MRI was able to accurately assess the volume of each fat pad of the mouse specifically. The change of FF value in WAT indirectly reflected the change of cellular properties in the tissue, proving the information on the browning effect of irisin in WAT. Noteworthy, the previous studies found that irisin induced browning of sWAT, but the role of irisin in vWAT has been controversial.[25] Interestingly, our study detected that irisin could induce browning in eWAT, even though the morphological changes of visceral lipid droplets were not significant in NCD mice. These findings demonstrated that adipose tissue exhibits a wide range of plasticity showing in different anatomical depots even in different layers of the same fat pad.[26] Therefore, the browning effect of irisin on WAT in different regions may have different underlying mechanisms. Consequently, MRI can be an important tool to be used sampling overall and individual tissue compartments in the future investigations.

We presented the preliminary findings of the effect of irisin on obesity at a low dose. It is likely that the irisin effect on the serum triglycerides may not be as sensitive as blood glucose and cholesterol in HFD animals. Fat decomposition and glucose decomposition are the regulating nodes of heat production and energy consumption of beige fat tissue. The liposoluble effect of lipid droplets has been widely studied in white adipocytes. The results show that lipid droplets directly provide fatty acids for Brown mitochondria to produce heat, which need to be supplemented by lipid fuel obtained from blood.[27] Fatty acids are the main chemical fuel for heat production of bat, while glucose can be converted into fatty acids through fat production.[28] Therefore, in the state of obesity and other imbalances, irisin's consumption of glucose in obese mice may make up for the consumption of triglycerides. In the future, we will use or include mouse models of diabetes to further verify the effect of irisin on metabolism.

There are a few limitations in the current study. Firstly, we did not investigate the delivery, accumulation and distribution of irisin in the tissue. In addition, the fat component change due to the effect of irisin was only monitored by noninvasive MRI in fairly short period (i.e. 14 days), thus the long-term effect is not fully investigated. Our follow-up studies in the future will seek better understanding of the effect of irisin on WAT by following up the medication and functional change with systematical and large cohort investigations on metabolic processes.

Irisin intervention exerts browning of WAT, resulting reduction of the WAT volume and decreased FF of WAT as measured by noninvasive MRI. Furthermore, it can improve the hyperglycemia in mice with diet-induced obesity. The findings from this study suggest that promoting the browning of WAT, as shown by irisin intervention, can be a new therapeutic approach to treat obesity or related metabolic disorders and diseases, such as diabetes.

Irisin can be used to activate and facilitate browning of WAT for treating obesity-related metabolic diseases and disorders. MRI is capable of noninvasively monitoring the process of WAT browning and the effect of irisin intervention.

AUTHORS' CONTRIBUTIONS

YC, XGP, JD, SHJ conceptualized the problem; YC, XGP developed an experimental method; YC, YFZ, XGP conducted the experiments; YC, XGP did a literature research; YC wrote the manuscript; YC, YFZ collected resources; HM, XGP reviewed and edited; XGP, SHJ supervised.

DECLARATION OF CONFLICTING INTERESTS

The authors declared no potential conflicts of interest with respect to the research, authorship, and/or publication of this article.

FUNDING

The author(s) disclosed receipt of the following financial support for the research, authorship, and/or publication of this article: This study was funded by the National Natural Science Foundation of China (81501523, 81871412); the Fundamental Research Funds for the Central Universities (2242019k30035); the Research Funds for "333 project" in Jiangsu province (LGY2017100).

ORCID iD

Xin-Gui Peng https://orcid.org/0000-0003-2988-5984

SUPPLEMENTAL MATERIAL

Supplemental material for this article is available online.

REFERENCES

1. Raajendiran A, Ooi G, Bayliss J, O'Brien PE, Schittenhelm RB, Clark AK, Taylor RA, Rodeheffer MS, Burton PR, Watt MJ. Identification of metabolically distinct adipocyte progenitor cells in human adipose tissues. *Cell Rep* 2019;**27**:1528–40
2. Dichamp J, Barreau C, Guissard C, Carriere A, Martinez Y, Descombes X, Pénicaud L, Rouquette J, Casteilla L, Plouraboué F, Lorsignol A. 3D analysis of the whole subcutaneous adipose tissue reveals a complex spatial network of interconnected lobules with heterogeneous browning ability. *Sci Rep* 2019;**9**:6684
3. Rodriguez Lanzi C, Perdicaro D, Landa M, Fontana A, Antoniolli A, Miatello R, Oteiza P. Vazquez Prieto MJTJonb Grape pomace extract

induced beige cells in white adipose tissue from rats and in 3T3-L1 adipocytes. *J Nutr Biochem* 2018;**56**:224–33
4. Wu J, Bostrom P, Sparks LM, Ye L, Choi JH, Giang AH, Khandekar M, Virtanen KA, Nuutila P, Schaart G, Huang K, Tu H, van Marken Lichtenbelt WD, Hoeks J, Enerbäck S, Schrauwen P, Spiegelman BM. Beige adipocytes are a distinct type of thermogenic fat cell in mouse and human. *Cell* 2012;**150**:366–76
5. Zhao L, Wang B, Gomez NA, de Avila JM, Zhu MJ, Du M. Even a low dose of tamoxifen profoundly induces adipose tissue browning in female mice. *Int J Obes (Lond)* 2020;**44**:226–34
6. Kristóf E, Klusóczki Á, Veress R, Shaw A, Combi ZS, Varga K, Győry F, Balajthy Z, Bai P, Bacso Z, Fésüs L. Interleukin-6 released from differentiating human beige adipocytes improves browning. *Exp Cell Res* 2019;**377**:47–55
7. Klusóczki Á, Veréb Z, Vámos A, Fischer-Posovszky P, Wabitsch M, Bacso Z, Fésüs L, Kristóf E. Differentiating SGBS adipocytes respond to PPARgamma stimulation, irisin and BMP7 by functional browning and beige characteristics. *Sci Rep* 2019;**9**:5823–34
8. Carobbio S, Guenantin AC, Samuelson I, Bahri M, Vidal-Puig A. Brown and beige fat: from molecules to physiology and pathophysiology. *Biochim Biophys Acta Mol Cell Biol Lipids* 2019;**1864**:37–50
9. Reza M, Subramaniyam N, Sim C, Ge X, Sathiakumar D, McFarlane C, Sharma M, Kambadur RJNc. Irisin is a pro-myogenic factor that induces skeletal muscle hypertrophy and rescues denervation-induced atrophy. *Nat Commun* 2017;**8**:1104
10. Kim H, Wrann CD, Jedrychowski M, Vidoni S, Kitase Y, Nagano K, Zhou C, Chou J, Parkman VA, Novick SJ, Strutzenberg TS, Pascal BD, Le PT, Brooks DJ, Roche AM, Gerber KK, Mattheis L, Chen W, Tu H, Bouxsein ML, Griffin PR, Baron R, Rosen CJ, Bonewald LF, Spiegelman BM. Irisin mediates effects on bone and fat via alphaV integrin receptors. *Cell* 2018;**175**:1756–68 *e1717*
11. Jeremic N, Chaturvedi P, Tyagi S. Browning of white fat: novel insight into factors, mechanisms, and therapeutics. *J Cell Physiol* 2017;**232**:61–68
12. Lourenco MV, Frozza RL, de Freitas GB, Zhang H, Kincheski GC, Ribeiro FC, Gonçalves RA, Clarke JR, Beckman D, Staniszewski A, Berman H, Guerra LA, Forny-Germano L, Meier S, Wilcock DM, de Souza JM, Alves-Leon S, Prado VF, Prado MAM, Abisambra JF, Tovar-Moll F, Mattos P, Arancio O, Ferreira ST, De Felice FG. Exercise-linked FNDC5/irisin rescues synaptic plasticity and memory defects in Alzheimer's models. *Nat Med* 2019;**25**:165–75
13. Boström P, Wu J, Jedrychowski MP, Korde A, Ye L, Lo JC, Rasbach KA, Boström EA, Choi JH, Long JZ, Kajimura S, Zingaretti MC, Vind BF, Tu H, Cinti S, Højlund K, Gygi SP, Spiegelman BM. A PGC1-α-dependent myokine that drives brown-fat-like development of white fat and thermogenesis. *Nature* 2013;**481**:463–68
14. Young MF, Valaris S, Wrann CD. A role for FNDC5/irisin in the beneficial effects of exercise on the brain and in neurodegenerative diseases. *Prog Cardiovasc Dis* 2019;**62**:172–78
15. O'Regan DP, Callaghan MF, Wylezinska-Arridge M, Fitzpatrick J, Naoumova RP, Hajnal JV, Schmitz SA. Liver fat content and T2*: simultaneous measurement by using breath-hold multiecho MR imaging at 3.0 T–feasibility. *Radiology* 2008;**247**:550–57
16. Peng X, Ju S, Fang F, Wang Y, Fang K, Cui X, Liu G, Li P, Mao H, Teng GJ. Comparison of brown and white adipose tissue fat fractions in ob, seipin, and Fsp27 gene knockout mice by chemical shift-selective imaging and 1H-MR spectroscopy. *Am J Physiol Endocrinol Metab* 2013;**304**:E160–167
17. Guiu B, Petit JM, Loffroy R, Ben Salem D, Aho S, Masson D, Hillon P, Krause D, Cercueil JP. Quantification of liver fat content: Comparison of Triple-Echo chemical shift Gradient-Echo imaging and in vivo proton MRn spectroscopy. *Radiology* 2009;**250**:95–102
18. Peng XG, Ju S, Qin Y, Fang F, Cui X, Liu G, Ni Y, Teng GJ. Quantification of liver fat in mice: comparing dual-echo Dixon imaging, chemical shift imaging, and 1H-MR spectroscopy. *J Lipid Res* 2011;**52**:1847–55
19. Kir S, White JP, Kleiner S, Kazak L, Cohen P, Baracos VE, Spiegelman BM. Tumour-derived PTH-related protein triggers adipose tissue browning and cancer cachexia. *Nature* 2014;**513**:100–04
20. Hou X, Zhang Y, Li W, Hu AJ, Luo C, Zhou W, Hu JK, Daniele SG, Wang J, Sheng J, Fan Y, Greenberg AS, Farmer SR, Hu MG. CDK6 inhibits white to beige fat transition by suppressing RUNX1. *Nat Commun* 2018;**9**:1023
21. Lee MW, Odegaard JI, Mukundan L, Qiu Y, Molofsky AB, Nussbaum JC, Yun K, Locksley RM, Chawla A. Activated type 2 innate lymphoid cells regulate beige fat biogenesis. *Cell* 2015;**160**:74–87
22. Mahgoub MO, D'Souza C, Al Darmaki R, Baniyas M, Adeghate E. An update on the role of irisin in the regulation of endocrine and metabolic functions. *Peptides* 2018;**104**:15–23
23. Emami MR, Alipoor E, Hosseinzadeh-Attar MJ. Irisin - A potential contributor of insulin resistance in kidney failure. *Eur J Intern Med* 2017;**44**:e22–e23
24. Zhang Y, Li R, Meng Y, Li S, Donelan W, Zhao Y, Qi L, Zhang M, Wang X, Cui T, Yang LJ, Tang D. Irisin stimulates browning of white adipocytes through mitogen-activated protein kinase p38 MAP kinase and ERK MAP kinase signaling. *Diabetes* 2014;**63**:514–25
25. Moreno-Navarrete JM, Ortega F, Serrano M, Guerra E, Pardo G, Tinahones F, Ricart W, Fernández-Real JM. Irisin is expressed and produced by human muscle and adipose tissue in association with obesity and insulin resistance. *J Clin Endocrinol Metab* 2013;**98**:E769–78
26. Chan M, Lim YC, Yang J, Namwanje M, Liu L, Qiang L. Identification of a natural beige adipose depot in mice. *J Biol Chem* 2019;**294**:6751–61
27. Wu N, Zheng B, Shaywitz A, Dagon Y, Tower C, Bellinger G, Shen CH, Wen J, Asara J, McGraw TE, Kahn BB, Cantley LC. AMPK-dependent degradation of TXNIP upon energy stress leads to enhanced glucose uptake via GLUT1. *Mol Cell* 2013;**49**:1167–75
28. Putri M, Syamsunarno MR, Iso T, Yamaguchi A, Hanaoka H, Sunaga H, Koitabashi N, Matsui H, Yamazaki C, Kameo S, Tsushima Y, Yokoyama T, Koyama H, Abumrad NA, Kurabayashi M. CD36 is indispensable for thermogenesis under conditions of fasting and cold stress. *Biochem Biophys Res Commun* 2015;**457**:520–25

(Received October 12, 2020, Accepted March 9, 2021)